Magnetic Resonance Imaging: Lumbosacral Lipoma

Masaki Komiyama, M.D., Akira Hakuba, M.D., Yuichi Inoue, M.D., Toshihiro Yasui, M.D., Hisatsugu Yagura, M.D., Mitsuru Baba, M.D., and Shuro Nishimura, M.D.

Department of Neurosurgery, Baba Memorial Hospital, Sakai, Osaka, and Departments of Neurosurgery and Radiology, Osaka City University Medical School, Osaka Japan

Komiyama M, Hakuba A, Inoue Y, Yasui T, Yagura H, Baba M, Nishimura S. Magnetic resonance imaging: lumbosacral lipoma. Surg Neurol 1987;28:259–64.

To evaluate the clinical efficacy of magnetic resonance imaging (MRI) of lumbosacral lipomas, the magnetic resonance images of nine patients were reviewed. T1- and T2-weighted spin echo sequences were used with a 0.5-T magnetic resonance system. The tethered or low-positioned conus medullaris, the lipoma itself, the lipoma–cord interface, the subarachnoid space, and hydromyelia were clearly disclosed. The nerve rootlets were not as clear. These results indicate the possible discontinuance of myelography and metrizamide computed tomography (CT) cisternography for such imaging. The diagnostic modalities of choice for lumbosacral lipoma imaging are plain spine films, plain CT scan, and MRI.

KEY WORDS: Lumbosacral lipoma; Magnetic resonance imaging; Computed tomography; Cisternography; Myelography

Recent advances in diagnostic neuroradiology have greatly been due to x-ray computed tomography (CT) and magnetic resonance imaging (MRI). The usefulness of MRI in diagnosing spinal cord lesions has been well documented in recent studies [7,13,15]. The lumbosacral (LS) lipoma is a particularly important spinal disease in pediatric neurosurgery. Although the timing of surgical intervention has long been controversial, early intervention has been advocated recently, even for neurologically intact patients, on the assumption that they will develop neurological deficits sooner or later [2,3,5,6,8,9,17,21]. Plain spine films and metrizamide CT cisternography are conventionally accepted as the most appropriate diagnostic modalities for LS lipomas [8,14,16]. From the neurosurgical point of view, however, preoperative observation of the lipoma–cord interface, nerve rootlets, and subarachnoid space is of vital importance. The authors review the usefulness of MRI of LS lipomas in preoperative, postoperative, and follow-up examinations, and discuss the possibility of discontinuing the use of myelography and metrizamide CT cisternography in favor of MRI to diagnose LS lipomas.

Address reprint requests to: M. Komiyama, M.D., Department of Neurosurgery, Baba Memorial Hospital, 244, Higashi 4, Hamadera-Funao-Cho, Sakai, Osaka 592 Japan.

Received January 13, 1987, accepted March 3, 1987.

Materials and Methods

During the past 2 years, nine patients with LS lipomas underwent MRI at our clinic. There were three males and six females, aged 1 month to 70 years; five were postoperative, the remaining four were preoperative (Table 1). Operative verification was obtained in seven cases (excluding cases 8 and 9). Plain x-ray films, plain CT scans, and MRI were performed in the preoperative cases. Generally, only MRI was performed in the postoperative cases. Myelography and metrizamide CT cisternography were not performed in any case but one (case 9), which was referred to our clinic only for magnetic resonance study.

The magnetic resonance scanner used was a 0.5-T superconducting system (Picker International, Cleveland, OH). T1- and T2-weighted spin echo (SE) pulse sequences were used; the repetition time and echo time for T1- and T2-weighted SE images was 600–1,000/40 msec and 2,000/120 msec, respectively. Sagittal and axial images of 1.0-cm thick slices were usually obtained. The following items were evaluated: (1) tethered or low-positioned conus medullaris, (2) lipoma–cord interface, (3) subarachnoid space and its relationship to the spinal cord, (4) hydromyelia, and (5) nerve rootlets.

Results

In all cases, tethered or low-positioned conus medullaris was clearly demonstrated (Figures 1*A*, 4*C* and *D*). Axial images were much more useful for demonstrating the lower extremity of the spinal cord than were sagittal images (Figures 1*B*, 2*B*, and 4*B*). In the postoperative cases, it was impossible to differentiate tethered from nontethered low-positioned conus medullaris.

0090-3019/87/$3.50

Table 1. *Patient Data*

Case no.	Sex	Age	Previous operation	Lipoma	Low conus	Meningocele	Syrinx
1	F	1 mo	–	+	+	–	–
2	F	3 yr	–	+	+	–	+
3	M	7 yr	+	–	+	–	–
4	F	8 yr	+	+	+	+	–
5	M	9 yr	+	+	+	+	+
6	F	12 yr	+	+	+	+	–
7	F	16 yr	+	+	+	–	–
8	M	38 yr	–	+	+	–	–
9	F	70 yr	–	+	+	–	–

Except for one postoperative case (case 3), lipomas were clearly demonstrated as high intensity areas on T1-weighted SE images (Figures 3*A* and 4*C*) and as almost the same or slightly lower intensity, in comparison with the spinal cord, on T2-weighted SE images (Figures 3*B* and 4*D*). There was no residual lipoma in case 3. The continuity of the lipoma from the intraspinal to the subcutaneous region was also clearly demonstrated (Figure 1*A*). There was no difference in signal intensity between the lipoma and either epidural fat or subcutaneous fat tissue (Figure 1*B*). On axial images, a low intensity band (line) was observed between the lipoma and spinal cord due to chemical shift (Figures 2*B* and 4*B*). Thus, the lipoma–cord interface was displayed as a low intensity band in all cases but one (case 3). In sagittal images this low intensity band was also noted immediately cephalad to the lipoma (Figure 3*B*).

In all cases, the subarachnoid space was clearly disclosed in relation to the spinal cord and the lipoma, especially on axial images. A meningocele was observed in three cases (cases 4, 5, and 6). On axial images, the meningocele was seen to bulge to the opposite side of the lipoma in all three cases. The cerebrospinal fluid (CSF) usually appeared as a low intensity area on T1-weighted SE images and as a high intensity area on T2-weighted images (Figures 3*A* and *B*). On sagittal T2-

Figure 1. *Case 7: A 16-year-old girl who had undergone surgery for lumbosacral (LS) lipoma at age 2. 1, lipoma; 2, epidural fat; 3, spinal cord, 4, CSF space.* **(A)** *Sagittal T1-weighted SE image clearly shows anatomical relationship of lipoma, spinal cord, epidural fat, and CSF space.* **(B)** *Axial T1-weighted SE image at level of arrow in* **(A)** *shows almost the same intensity for lipoma and epidural fat. Relationship of CSF space, spinal cord. lipoma, and epidural fat are easily discerned. The ventral rootlet (arrowhead) is clear.*

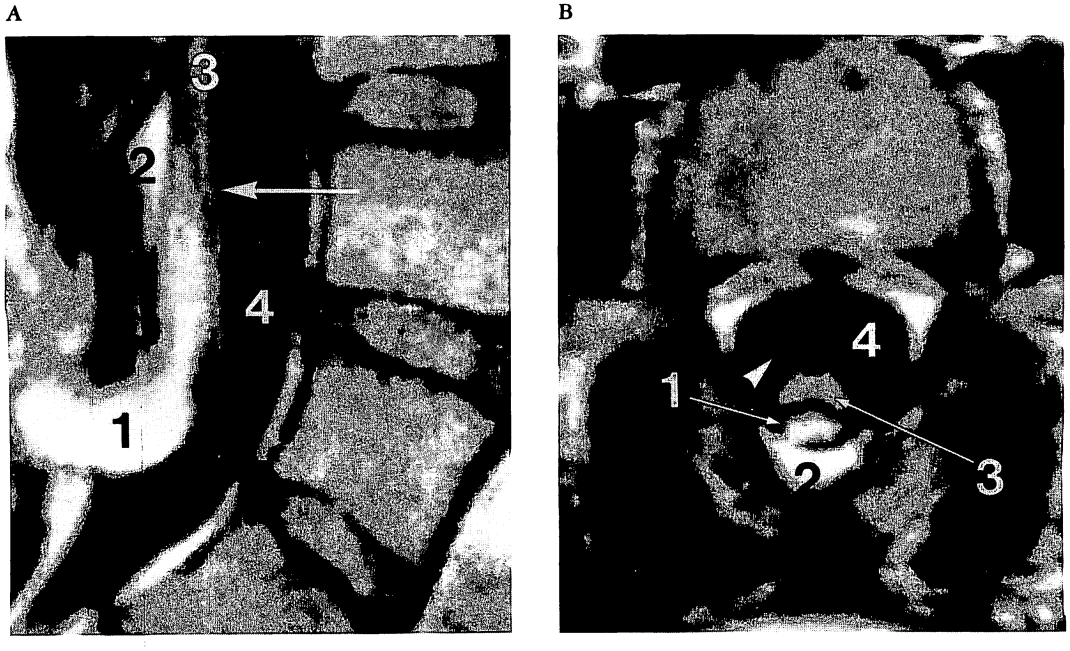

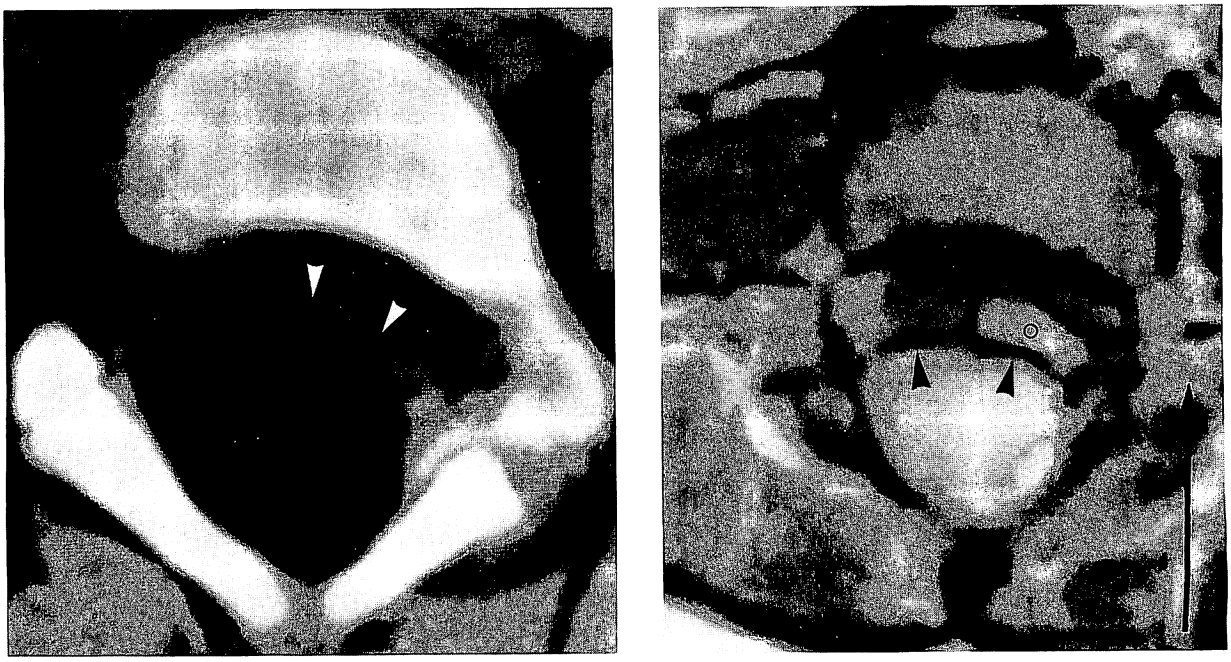

A B

Figure 2. *Case 2: A preoperative 3-year-old girl with LS lipoma.* **(A)** *Noncontrast CT demonstrates low attenuation of the lipoma at the L-5 level. Tethered spinal cord (arrowheads) is vaguely discernible at the anterolateral aspect of the lipoma.* **(B)** *Axial T1-weighted SE image clearly discloses both lipoma and spinal cord (circle). Note the low intensity band (arrowheads) due to chemical shift at the anterior aspect of the lipoma. Direction of frequency-encoding gradient (arrow) is from patient posterior to anterior. Lipoma image shifts in the direction opposite that of the frequency-encoding gradient.*

Figure 3. *Case 9: A 70-year-old woman with no previous surgery for LS lipoma.* **(A)** *Sagittal T1-weighted SE and* **(B)** *sagittal T2-weighted SE images. Arrows indicate direction of frequency-encoding gradient. Square, lipoma; white arrowhead, CSF cephalad to lipoma; black arrowhead, chemical shift artifact. On the T1-weighted SE image, the lipoma is of high intensity and the CSF is of low intensity. On the T2-weighted SE image, the CSF (white arrowhead) is of high intensity due to a long T2 value. However, the remainder of the CSF cavity is of relatively low intensity due to a CSF flow void effect. Immediately cephalad to the lipoma, a low intensity band due to chemical shift is noted.*

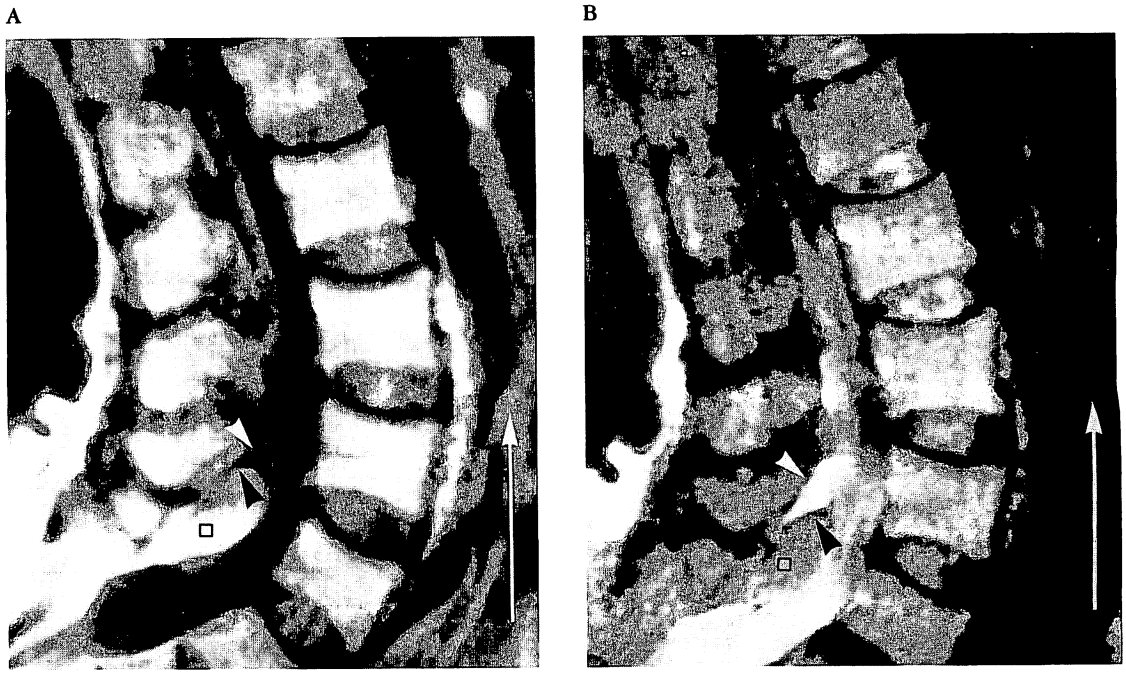

A B

Figure 4. *Case 5: A 9-year-old boy who had undergone previous surgery for LS lipoma at age 5.* **(A)** *Noncontrast CT scan demonstrates low attenuation of lipoma at right side of spinal column at the L-4/5 level. Spinal cord with hydromyelia (arrow) is vaguely discernible; it would be difficult to firmly diagnose a hydromyelia based on this image alone.* **(B)** *Axial T1-weighted SE image clearly demonstrates spinal cord with hydromyelia (arrowhead) as well as lipoma. The CSF space is also clearly shown. Note lipoma–cord interface, which appears as a low signal intensity area due to chemical shift.* **(C)** *Sagittal T1-weighted SE image discloses lipoma (square) of high, CSF of low, and the spinal cord (arrowheads) of intermediate intensity.* **(D)** *Sagittal T2-weighted SE image discloses lipoma (square) of intermediate and spinal cord of slightly higher intensity. The tethered spinal cord (arrowheads) is well displayed. Due to the CSF flow void effect, CSF ventral to the tethered spinal cord appears as a low intensity area, whereas the CSF at the level of the lipoma appears as a high intensity area.*

weighted SE images, however, the CSF appeared as an area of relatively low intensity (Figure 4*D*). This occurred mainly in the CSF ventral to the spinal cord in the LS region.

Hydromyelia, noted in two cases (cases 2 and 5), appeared as a low intensity area on T1-weighted SE images (Figure 4*B*). The relationship between hydromyelia and subarachnoid space was not clearly disclosed.

The nerve rootlets at the level of the lipoma were often, though not always, demonstrated on the ventrolateral part of the low-positioned conus on axial images (Figures 1*B* and 5).

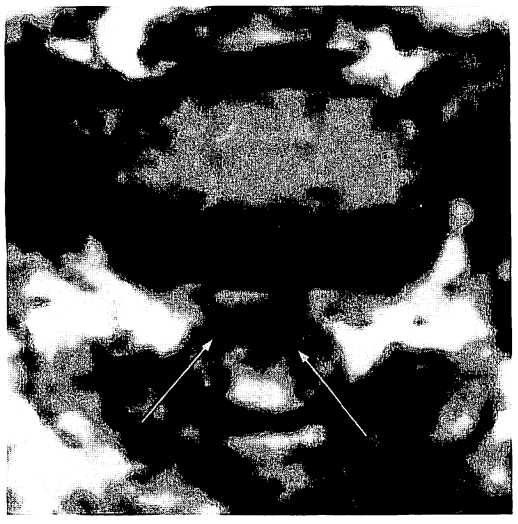

Figure 5. *Case 3: A 7-year-old boy who had undergone surgery for LS lipoma at age 3. Axial T1-weighted SE image clearly shows ventral rootlets (arrows) due to myeloschisis. Dorsal rootlets, however, are not identified. Since the lipoma has been totally removed, no residual lipoma is seen.*

Discussion

For diagnosis of the LS lipoma, plain spine films and metrizamide CT cisternography are the conventionally accepted modalities of choice [8,14,16]. Spina bifida and its related bony abnormalities are commonly diagnosed via plain film. Plain CT scan remains of value because it is essentially noninvasive and demonstrates the lipoma well [20].

As to the utility of myelography in the preoperative examination, Lassman and James [9] comment that it is essential to the final diagnosis. However, Caram et al [4] reported aggravation of clinical signs following lumbar puncture in two lipoma cases. Loeser and Lewin [11] reported unsuccessful lumbar myelography and conclude that any patient with spina bifida occulta, LS subcutaneous lipoma, or neurological deficit should be studied via the cisternal route, as the conus and intradural tumor might completely fill the lumbar theca. Bruce and Schut [3] reported that no complications occurred and no evidence of Chiari malformation was found in their 35 cases of lipoma in which cisternal myelography was used. They conclude that myelography should be performed in all cases of lipoma, either via the cisternal or the lateral cervical technique. Hoffman et al [8] reported no Chiari malformation in their 97 cases of lipomyelomeningoceles. On the other hand, Naidich et al [14] reported one lipomyeloschisis with Chiari I malformation, which had low-positioned cerebellar tonsils at C-2. Although the incidence of Chiari malformation in LS lipomas may be low, it is, nevertheless, desirable to avoid cisternal or lateral cervical puncture for fear of possible asymptomatic Chiari malformation [12].

Myelographic findings such as large dural sac, low-positioned conus medullaris, thick film terminale, extradural or intradural mass, horizontal or cephalad nerve rootlets, and meningocele can be demonstrated as accurately through MRI as through myelography, and on some occasions, possibly better. Moreover, conventional myelography sometimes misses lipomas [16,19]. Also, the lower extremity of the subarachnoid space is occasionally highly terminated due to the mass of the lipoma [5,6]. In these instances, it is meaningless to perform either myelography or metrizamide CT cisternography, because neither can demonstrate the anatomy around the lipoma, which is of the utmost concern. The dural sac may end at the LS junction, and lack of caudal filling to this point may be mistaken as representing high dural sac termination rather than a true filling defect [19].

Despite the utility of metrizamide CT cisternography [16], it is principally invasive and therefore includes the risk of neurological deterioration resulting from cisternal puncture and possible morbidity attributable to metrizamide.

MRI discloses lipomas as high intensity areas on T1-weighted SE images and as intermediate intensity areas on T2-weighted SE images. This is due to the short T1 (longitudinal relaxation times) and the relatively short T2 (transverse relaxation times) of the fat tissue. The lipoma has the same intensity as epidural and subcutaneous fat tissues, because it also is adult adipose tissue.

Protons in the fat tissues have slightly different resonating frequencies from those in nonfat tissues; this phenomenon, called chemical shift, produces the image artifact on magnetic resonance images [22]. In our system, a fat image shifts about 1.5 pixels with respect to a water (nonfat) image in the direction of lower frequency-encoding gradient. In axial images, the direction of frequency-encoding gradient is from patient posterior to anterior, and in sagittal images from caudal to cephalad, in our system. Thus, the low intensity band is usually anterior to the fat tissue in axial images and cephalad in sagittal images. This chemical shift appears at the lipoma–cord interface in axial images, in our system. Although we can use this chemical shift artifact as a landmark of the interface, this low intensity band is the expression of pixel misregistration; its width is not the true width of the lipoma–cord interface, but the degree of the chemical shift itself.

The CSF appears essentially as a low intensity area on T1-weighted SE images and as a high intensity area on T2-weighted images, due to its long T1 and T2 values; a dilated CSF space such as a meningocele is thus disclosed without contrast medium. The CSF occasionally, however, appears as a lower than usual intensity due to a flow void effect, which occurs as a result of the

rapid, pulsatile flow of the CSF; this is seen more often on T2-weighted than on T1-weighted SE images [18].

Metrizamide CT cisternography often demonstrates a hydromyelia or a syringomyelia more accurately than noncontrast CT [1], but it is usually disclosed via MRI; its extension in the spinal axis can also be recognized [7,10,13,15]. MRI is as accurate as metrizamide CT cisternography in the diagnosis of intramedullary cavities that result in spinal cord enlargement, but is less sensitive in detecting cavities within normal-sized or diminished spinal cords [10].

In conclusion, the diagnostic modalities of choice in LS lipoma are plain films, plain CT scans, and MRI, as well as urological examination: thus, the lumbar or cisternal puncture necessary for either myelography or metrizamide CT cisternography may be eliminated for safer examination.

The authors are grateful to K. Ishii and S. Maeda for their assistance in the preparation of the manuscript.

References

1. Aubin ML, Vignaud J, Jardin C, Bar D. Computed tomography in 75 clinical cases of syringomyelia. AJNR 1981;2:199–204.
2. Bassett RC. The neurologic deficit associated with lipomas of the cauda equina. Ann Surg 1950;131:109–16.
3. Bruce DA, Schut L. Spinal lipomas in infancy and childhood. Child's Brain 1979;5:192–203.
4. Caram PC, Scarcella G, Carton CA. Intradural lipomas of the spinal cord. J Neurosurg 1957;14:28–41.
5. Chapman PH. Congenital intraspinal lipomas. Child's Brain 1982;9: 37–47.
6. Hakuba A, Fujitani K, Hoda K, Inoue Y, Nishimura S. Lumbosacral lipoma, the timing of the operation and morphological classification. Neuro-orthopedics 1986;2:34–42.
7. Han JS, Kaufman B, El Yousef SJ, Benson JE, Bonstelle CT, Alfidi RJ, Haaga JR, Yeung H, Huss RG. NMR imaging of the spine. AJNR 1983;4:1151–9.
8. Hoffman HJ, Taecholarn C, Hendrick EB, Humphreys RP. Management of lipomyelomeningoceles. J Neurosurg 1985;62:1–8.
9. Lassman LP, James CCM. Lumbosacral lipomas: critical survey of 26 cases submitted to laminectomy. J Neurol Neurosurg Psychiatry 1967;30:174–81.
10. Lee BCP, Zimmerman RD, Manning JJ, Deck MDF. MR imaging of syringomyelia and hydromyelia. AJNR 1985;6:221–8.
11. Loeser JD, Lewin RJ. Case reports and technical note, lumbosacral lipoma in the adult. J Neurosurg 1968;29:405–9.
12. Malis LI. Intramedullary spinal cord tumors. Clin Neurosurg 1978;25:512–39.
13. Modic MT, Weinstein MA, Pavlicek W, Starnes DL, Duchesneau PM, Boumphrey F, Hardy RJ Jr. Nuclear magnetic resonance imaging of the spine. Radiology 1983;148:757–62.
14. Naidich TP, McLone DG, Mutluer S. A new understanding of dorsal dysraphism with lipoma (lipomyeloschisis): radiologic evaluation and surgical correction. AJNR 1983;4:103–16.
15. Norman D, Mills CM, Brant-Zawadzki M, Yeates A, Crooks LE, Kaufman L. Magnetic resonance imaging of the spinal cord and canal: potentials and limitations. AJR 1983;141:1147–52.
16. Resjö IM, Harwood-Nash DC, Fitz CR, Chuang S. Computed tomographic metrizamide myelography in spinal dysraphism in infants and children. J Compt Assist Tomogr 1978;2:549–58.
17. Rogers HM, Long DM, Chou SN, French LA. Lipomas of the spinal cord and cauda equina. J Neurosurg 1971;34:349–54.
18. Sherman JL, Citrin CM. Magnetic resonance demonstration of normal CSF flow. AJNR 1986;7:3–6.
19. Swanson HS, Barnett JC Jr. Intradural lipomas in children. Pediatrics 1962;29:911–26.
20. Tsumura M, Takemoto K, Fukuda T, Minamikawa Y, Oda J, Inoue Y, Onoyama Y, Hakuba A, Hoda K, Umekawa T, Fujitani K. Computed tomography of spinal lumbosacral lipoma in children. Jpn J Clin Radiol 1983;28:1569–73.
21. Villarejo FJ, Blazquez MG, Gutièrrez-Diaz JA. Intraspinal lipomas in children. Child's Brain 1976;2:361–70.
22. Weinreb JC, Brateman L, Babcock EE, Maravilla KR, Cohen JM, Horner SD. Chemical shift artifact in clinical magnetic resonance images at 0.35 T. AJR 1985;145:183–5.